IEEE Access
Multidisciplinary | Rapid Review | Open Access Journal

Received 11 December 2023, accepted 22 December 2023, date of publication 25 December 2023,
date of current version 3 January 2024.

Digital Object Identifier 10.1109/ACCESS.2023.3347336

RESEARCH ARTICLE

A Novel Fast ICA-FBCCA Algorithm and Convolutional Neural Network for Single-Flicker SSVEP-Based BCIs

SEYEDEH NADIA AGHILI[1], SEPIDEH KILANI[1], EHSAN ROUHANI[2], AND AMIR AKHAVAN[2]
[1]Department of Electrical and Computer Engineering, Iran University of Science and Technology, Tehran 16846-13114, Iran
[2]Department of Electrical and Computer Engineering, Isfahan University of Technology, Isfahan 84156-83111, Iran

Corresponding author: Ehsan Rouhani (erouhani@iut.ac.ir)

This work involved human subjects or animals in its research. Approval of all ethical and experimental procedures and protocols was granted by the Ethics Committees of Iran's Medical Sciences and Medical Association, Hamburg, Germany.

ABSTRACT Brain-computer interface (BCI) systems have been developed to assist individuals with neuromuscular disorders to communicate with their surroundings using their brain signals. One attractive branch of BCI is steady-state visual evoked potential (SSVEP), which has acceptable speed and accuracy and is non-invasive. However, SSVEP-based EEG signals suffer from eye-fatigue problems, resulting in artifacts that affect the accuracy of the system. Thus, researchers are still working to improve SSVEP-based BCI systems. This paper proposes robust machine-learning algorithm for single-flicker SSVEP detection. A novel approach based on fast independent component analysis and filter-bank canonical correlation analysis (fast ICA-FBCCA) is developed to extract features from the single-flicker SSVEP signal. The clean features learned by fast ICA-FBCCA are then applied to a discrete wavelet transform (DWT) technique and fed to a convolutional neural network (CNN) with only one convolutional layer and a smaller number of parameters. The effectiveness of the proposed technique is evaluated using two datasets. The results were evaluated using two datasets. The findings clearly demonstrate that the proposed method outperforms traditional methods, with average target recognition accuracy and standard deviation values of $97 \pm 3.1\%$ among 6 subjects for dataset 1 and $82.12 \pm 10.7\%$ among 12 subjects for dataset 2. Overall, these findings suggest that the proposed method is a promising approach for improving the accuracy and reliability of the single-flicker SSVEP-based BCI systems.

INDEX TERMS Brain–computer interface (BCI), single-flicker steady-state visual evoked potential, fast independent component analysis (fast ICA), filter-bank canonical correlation analysis (FBCCA), convolutional neural network (CNN).

I. INTRODUCTION

Brain-computer interface (BCI) is a communication device that allows individuals to control computers or other devices using their brain signals, thereby enabling communication or control without the need for muscle movement [1], [2]. The primary objective of research and advancement in the field of BCIs is to develop an innovative communication tool that can be used specifically for people who have experienced stroke, neurological disorders, muscle impairment, or spinal cord injuries. These individuals face significant challenges in effectively engaging with their environment using conventional communication methods, necessitating the development of alternative means to facilitate their communication capabilities. BCIs enable individuals to issue commands directly to a computer, robot, or smart prosthesis through their brain signals. The important application of BCI performed by machine learning (ML) is device control such as wheelchairs [3], robots [4], car [5], cursor [6], and spellers [7]. Various techniques are used to measure brain

The associate editor coordinating the review of this manuscript and approving it for publication was Giacinto Barresi.

activity in BCIs, predominantly relying on the acquisition of electrical signals via invasive or non-invasive approaches. Invasive methods involve the insertion of electrodes either intracranially, or on the surface of the cortex, while non-invasive approaches employ specialized scalp sensors to receive electrical waves and hence are more suitable for human experiments. Electroencephalogram (EEG) is often used for measuring non-invasive brain signals in BCI applications such as steady-state visual evoked potential (SSVEP) [8], [9], P300-based event-related potential (ERP) [10], [11], sensorimotor rhythm (SMR) [12], and slow cortical potential (SCP) [13]. SSVEP is of great interest due to its high communication rate, making it well-suited for spelling systems where a high information transfer rate (ITR) is crucial [14].

SSVEP signals refer to periodic visual cortical responses that occur in the occipital cortex in response to visual flicker stimulation at specific frequencies. A typical SSVEP graphical user interface (GUI) consists of various visual positions (stimuli) set at fixed frequencies. When individuals pay attention to these stimuli, the power in their EEG signal increases, which can be used as a feature in signal processing [15], [16]. Nevertheless, employing a GUI featuring multiple frequencies can potentially induce visual strain and increase eye fatigue [17]. To address this, some SSVEP-based BCIs employ a single-flicker frequency for multiple stimulus. Single-flicker SSVEP is a novel BCI that uses only one flickering stimulus to generate multiple commands from the user's brain signals [18], [19]. It is based on the principle of retinotopic mapping, which means that the brain response depends on the spatial position of the stimulus relative to the center of gaze [20]. Although it reduces visual fatigue, improves the signal-to-noise ratio, and enhances the spatial attention mechanism of the brain, it can be more sensitive to eye movements and blinks, and more affected by individual differences in retinotopic mapping. Consequently, the design of algorithms for single-flicker SSVEP presents certain obstacles, including determining the optimal stimulus design, selecting appropriate features and classifiers, and calibrating and customizing the system for each user [19], [21], [22]. Furthermore, there is currently a dearth of available datasets and suitable algorithms for analyzing this type of signal. The primary objective of this study is to investigate the shortage of comparative algorithmic research and develop effective solutions to address this issue. These systems' effectiveness relies heavily on the ability to extract the most relevant features and classification accuracy. Therefore, identifying the optimal algorithm for analyzing this type of SSVEP signal can be a significant step toward developing more effective and user-friendly single-flicker SSVEP-based BCIs.

The selection of an appropriate feature extraction technique plays an important role to enhance the accuracy and reliability of the system's performance in a single-flicker frequency SSVEP-based BCIs. Power spectral density analysis (PSDA) is one of the earliest technique used for SSVEP analysis [19], [20], [23]. However, the PSDA has limited application due to the sensitivity of the SSVEP signal to noise and the low-frequency resolution in short-time windowing [24]. Furthermore, PSDA does not consider the spatial information of the EEG signal, which makes it less suitable for single-flicker SSVEP analysis. The results of Lin et al. [23] on multiple subjects showed the high performance of the canonical correlation analysis (CCA) in feature learning of SSVEP signals in comparison with the PSDA approach. The CCA finds the linear composition of channels to maximize the correlation between the two multidimensional signals (reference signal and EEG signal). Filter bank CCA (FBCCA) [25] has been proposed as a powerful spatial filter for analyzing single-flicker SSVEP signals, with the ability to utilize harmonic frequency information to enhance the CCA. FBCCA is a powerful method that decomposes a signal with multiple filters into different sub-bands and performs CCA on each sub-band. To extract more distinct and appropriate features with more details, especially in temporal and frequency domains, discrete wavelet transform (DWT) can be used to reduce the amount of data required for SSVEP analysis. This can make the analysis faster and more efficient. Moreover, this technique is used to identify and remove artifacts (such as ocular artifacts) from the SSVEP signal and can improve the accuracy of the analysis. Nonetheless, the method may not be able to effectively remove artifacts in situations where there is an overlap between the signal spectrum, which can limit its effectiveness in some cases [26]. The regression methods are widely used in ocular removal artifacts [27]. But this technique severs several limitations for the practical application of BCI-based systems such as computational complexity [28] and the need for a suitable reference signal (e.g., electrooculographic channel (EOG) in ocular removal [29]). To overcome the lack of an extra reference signal, blind source separation (BSS) techniques such as independent component analysis (ICA), and CCA have been suggested [30], [31]. Fast ICA is a more flexible method that has been widely used to remove separate artifacts such as eye blinks by constructing a new mixture of sources [32], [33]. Although the fast ICA reduces the computational complexity in real-time and makes BCI applications more accurate [34], this technique does not effectively eliminate artifacts with variable spatial distribution such as electromyography (EMG) [35]. The CCA has been proposed as an alternative approach to remove EMG artifacts from EEG [36]. Due to the similarity of the nature of the EMG signals to white noise (low autocorrelation coefficient), CCA is used to remove the EMG artifacts by extracting the independent sources with maximum autocorrelation coefficient [37]. The current study has combined the fast ICA with the filter-bank CCA (FBCCA) to generate a clean signal and optimally extract spatial features for single-flicker SSVEP signals, offering a comparison between FBCCA and traditional CCA method for feature extraction purposes. Furthermore, following the extracted optimal spatial features by a combination of the fast ICA and FBCCA, the DWT is used to reduce the sample size and make a tradeoff between the time and frequency resolution [38].

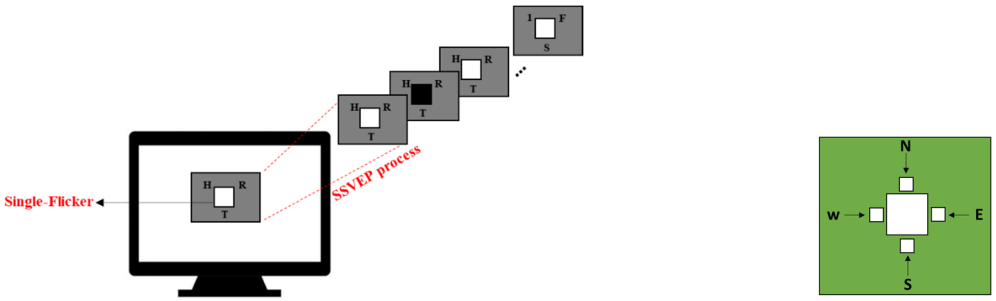

(a) (b)

FIGURE 1. Overall schematic of the BCI speller protocol related to (a) Dataset 1 and (b) Dataset 2. In (a), the following steps are performed in the experimental run: First, three characters to be spelled in that run are displayed for 2 seconds. Next, the target character for the trial is displayed for another 2 seconds. Then, a sequence of 45 stimuli is presented, with 9 groups repeated 5 times each. At the same time, a white square at the center of the screen is flickering at 15 Hz. The subject sits in front of a monitor and the EEG signals are acquired by the EEG-recorded device and its accessories (including 10-20 EEG caps, and electrodes). Then, the collected data is processed during experiments with 24 offline runs. In (b), a flickering square at 15 Hz was presented at the center and the indicated small white squares (N, W, S, and E) prompt participants to focus their gaze, causing landscape movement in the respective direction. During training, the target was highlighted in red. The participants looked at the N target where N for the Dataset 1 and 2 is set to be 3 and 4, respectively.

The next step in the single-flicker SSVEP detection algorithm involves the classification of the extracted features. Previous studies has employed conventional classifiers for target detection in SSVEP analysis and have demonstrated improved performance by leveraging deep learning (DL) techniques [39], [40], [41]. Convolutional neural network (CNN) is a widely used deep learning (DL) approach for extracting feature representations in image classification problems [42], [43], [44], and its capacity for discovering invariant features has shown potential for enhancing methods applied in EEG signal analysis [45], [46], [47], [48]. Recently, CNN has attracted attention in SSVEP-based EEG [41], [49], [50], [51] and demonstrated higher performance in comparison with other traditional classifier methods [39], [40], [41] such as the CCA (when used as the classifier [3], [52]), neural network (NN), k-nearest neighbor (K-NN), linear discriminant analysis (LDA), and support vector machine (SVM) methods. Moreover, CNN has advantages including (i) local connections [53], (ii) extract hierarchical features by sharing the weights [54], and (iii) pooling and the use of many layers [55]. However, the large number of parameters makes it a problem to realize the real-time implementation of such DL models. Ensuring real-time processing is crucial for practical applications, as delayed responses can hinder user experience and usability. Actually, it enables smooth interaction with the environment. However, as mentioned, most DL models require parameters in their structure. Therefore, the current study tries to introduce a new approach for CNN (as a classifier) with a small number of parameters. In this paper, we present a novel ML algorithm for SSVEP detection that introduces several innovative features, including:

- A novel hybrid feature extraction approach is introduced. This method combined the fast ICA with FBCCA to extract spatial features from the single-flicker SSVEP signal. Additionally, DWT is used for dimension reduction and to make a trade-off between time and frequency resolution before the classification stage.
- A novel CNN classification architecture is proposed, which employs temporal convolution for identifying distinct target classes in EEG signals. This represents the first implementation of deep neural networks (DNN) in single-flicker SSVEP based systems.
- To the best of our knowledge, this study provides the opportunity for the first time to consider and compare several traditional methods for single-flicker SSVEP.

The effectiveness of the proposed single-flicker SSVEP-based BCI technique is evaluated on two BCI dataset [20], [56], and the results are compared with previous works. The obtained results demonstrate reliable classification.

II. MATERIALS AND METHOD

A. DATASET AND PREPROCESSING

1) DATASET 1

All BCI experiments performed in [56] were used in the current study which are approved by the Ethics Committees of Iran's Medical Sciences. The experiments were carried out in accordance with the relevant guidelines and regulations. All participants provided written informed consent according to the institutional guidelines for datasets. Fig. 1(a) illustrates the overall schematics of the BCI speller protocol related to the RSVP-single flicker SSVEP dataset. The dataset was obtained by recording data from six subjects (male, aged 22–27, mean 24.8) who participated in the rapid serial visual presentation (RSVP)-single-flicker SSVEP paradigm using a BCI speller [56]. The visual stimulus consists of 27 letters arranged into nine groups, with each group containing three distinct letters that are encircled by a single flickering square that blinks at a frequency of 15 Hz. The nine groups of letters are displayed randomly on the screen five times (repetitions) as visual stimuli. This repeated presentation ensures comprehensive data collection and robust analysis. The approach

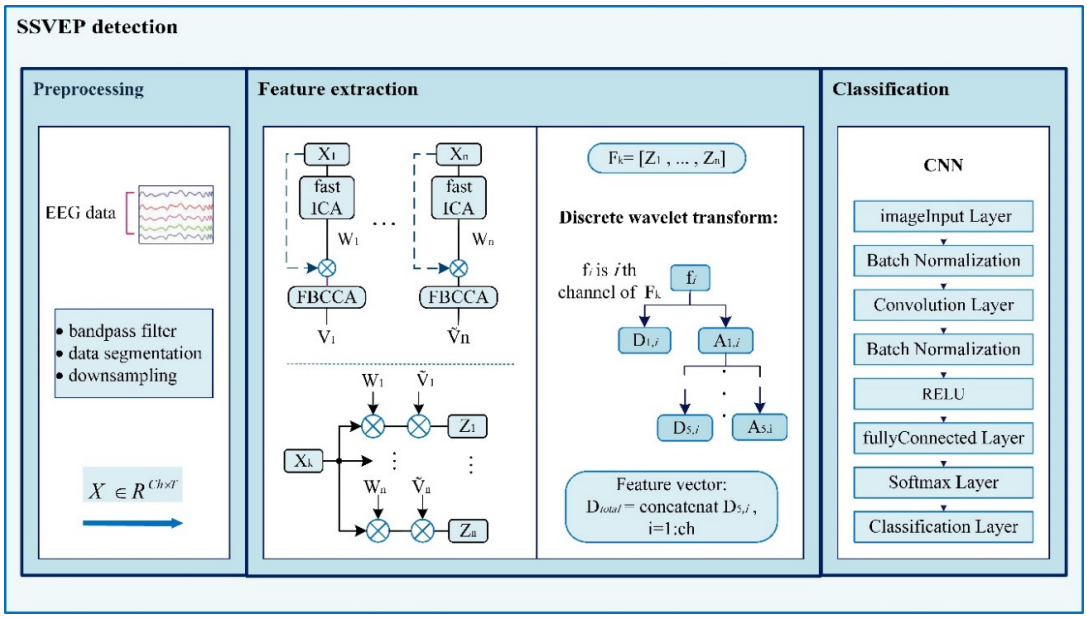

FIGURE 2. Overview of the proposed method. The methodology comprises three stages: preprocessing, feature extraction, and classification. In the preprocessing stage, EEG data undergoes band-pass filtering and epoch segmentation. The feature extraction phase employs a hybrid fast ICA-FBCCA technique with mapping weights (W, V) and then the discrete wavelet transforms. Finally, in classification stage, the extracted features feed into a CNN for target character detection.

outlined in this protocol involves a fusion of the RSVP and single-flicker SSVEP techniques. By leveraging the single-flicker SSVEP attributes, the system identifies the target direction, while the utilization of the RSVP protocol, which triggers a P300 response, facilitates the recognition of the target stimulus. In the experiment, each participant completed a total of 24 offline runs. Each run consisted of three trials, with each trial involving the spelling of three characters. During each trial, a total of 45 stimuli were presented to the participant. The subject sits in front of the monitor and focuses on the task. The electrodes were placed on the head and recorded the EEG signals from 32-channel g.Hlamp device at a sampling rate of 512 Hz. The right earlobe electrode was designated as the reference channel, while the forehead electrode was considered as the ground (GND). This study utilized only a single-flicker SSVEP signals for evaluation that consist of 3 targets (related to three characters surrounded by 15 Hz flickering square at the center of the screen). For the analysis of single-flicker SSVEP signals, 10 channels (P7, P3, Pz, P2, P8, PO7, PO3, PO4, PO8, and Oz in the international 10-20 system) were selected according to [56] which they covered the occipital and parietal regions. The EEG signals were filtered using a 1-47 Hz band-pass filter and segmented into 10.5 s epochs in the preprocessing step. The extracted SSVEP signals were then fed into the feature extraction block.

2) DATASET 2

All BCI experiments performed in ref. [20] were used in the current study which are approved by the ethics committee of the medical association of the city of Hamburg, Germany.This dataset comprises recordings from 12 participants who engaged in the single-flicker SSVEP paradigm utilizing a BCI setup as detailed in [20]. The experiments were carried out in accordance with the relevant guidelines and regulations. All participants provided written informed consent according to the institutional guidelines for datasets. As depicted in Fig. 1(b), a flickering square at a frequency of 15 Hz was displayed, eliciting SSVEP responses from the participants. Four smaller squares were positioned around the flickering square, serving as target classes for participants to focus their gaze on (please refer to [20] for more specifics). The EEG signals were captured using the 32-channel BioSemi ActiveTwo AD-box (BioSemi Instrumentation, Amsterdam, The Netherlands) with a high sampling rate of 2048 Hz. All recording channels were employed for SSVEP signal analysis. During the preprocessing stage for SSVEP, the EEG signals were filtered via a band-pass filter set at 1-80 Hz and were subsequently segmented into epochs lasting 3.5 seconds each. Subsequently, the data were downsampled to a frequency of 512 Hz.

B. THE PROPOSED ARCHITECTURE FOR SINGLE-FLICKER DETECTION

The proposed method consists of three main phases: preprocessing, feature extraction, and classification, as illustrated in Fig. 2. The EEG data is first filtered using a band-pass filter and subsequently, the filtered signals are segmented into epochs. The preprocessed signals are then fed into the feature extraction stage ($X = R^{Ch \times T}$) where Ch and T denote spatial and temporal features, respectively. In the second phase, the features from the preprocessed data are extracted using the new hybrid fast ICA-FBCCA technique by two mapping weights (W, V) followed by the DWT technique. Finally, the

new CNN architecture is proposed for detecting the target character. All analyses are performed by MATLAB R2019b.

1) FEATURE EXTRACTION

In the SSVEP protocol, high artifacts due to eye fatigue problems are a troubling issue for real-time implementation. ICA is a flexible method that has been widely used to remove separate artifacts by constructing a mixture of sources [32], [33]. However, the fast ICA reduces the computational complexity in real-time and makes BCI applications more accurate [34] compared to ICA. Hence, the fast ICA-based blind source separation algorithm is utilized to remove these kinds of artifacts. The fast ICA algorithm is based on the maximization entropy principle across the channels (Ch). Therefore, a total of N training classes (related to N different directions in single-flicker SSVEP GUI, denoted as $X_c, c = 1, 2, ..,N$) are fed to fast ICA process. This results in the derivation of N weights (designated as $W_c, c = 1, 2, ..,N$) intended to purify the single-flicker SSVEP signal by removing artifacts ($\tilde{X}_c = W_c \times X_c, c = 1, 2, ..,N$). Furthermore, since there are different characters in the different regions surrounding the single-flicker stimulus (15 Hz), their spatial properties change in different regions of the brain accordingly [56]. FBCCA is an efficient spatial filter to make more discriminative the N difference classes. Hence, it is applied to the output of the fast ICA method to extract the spatial features. The FBCCA is a modified CCA to incorporate fundamental and harmonic frequency components and consists of two steps including (1) the filter and (2) the CCA. Firstly, a filter bank analysis divides the signal into distinct passbands, indicated by "I", achieved through sub-band decompositions using multiple filters. Secondly, in the CCA step, it finds projection matrices $\tilde{V}$ and B for each sub-band to maximize the canonical correlations ($\rho = [\rho_1, \ldots, \rho_M]$) between $\tilde{V}\tilde{X}_c$ and BY where $\tilde{X}_c$ and Y are modified signals by fast ICA and reference signals, respectively. The ith canonical correlation is calculated as $\rho_i = \rho(\tilde{V}(i)\tilde{X}_c, B(i)Y)$ which the number of canonical variables is $M = min\left(rank\left(\tilde{X}_c\right), rank(Y)\right)$. The reference signals are created by a sinusoidal-cosine signal of 15 Hz and its 10 harmonics as follows [56]:

$$Y = [\sin(2\pi ft); \cos(2\pi ft); \sin(4\pi ft); \cos(4\pi ft); \ldots; \sin(10\pi ft); \cos(10\pi ft)] \quad (1)$$

where f is the stimulation frequency (15 Hz) and t is the number of data samples. In the current study, the projection matrices $\tilde{V}_c$ and B_c are calculated for each class ($c = 1, 2, ..,N$). Subsequently, for K trials, each sample of the modified signal through fast ICA, denoted as $\tilde{X}_{c,k} = W_k \times X_{c,k}$ where $k = 1, \ldots, K$, is then multiplied by $\tilde{V}_c$ to yield $z_{c,k} = \tilde{V}_c \times \tilde{X}_{c,k}$. Finally, the elements of $z_{c,k} (c = 1, 2, ..,N)$ are concatenated into the form of $F_k = [z_1\ z_2, \ldots,\ z_k]$ to achieve a high-level clean SSVEP signal. The fast ICA-FBCCA code description is given below in Algorithm 1.

In the next phase of feature extraction, DWT is used to reduce the sample size and improve frequency resolution. It decomposes the signal into a coarse approximation and detail information by filtering the input vector through a series of low- and high-pass filters, respectively. The signals are decomposed into different frequency bands, and then, the features with more information are selected. The one level of decomposition for input L is performed by applying a high-pass filter $g[.]$, and a low-pass filter $h[.]$ to each channel vector of L (i.e. $b[n]$) as follow:

$$D_1[k] = \sum_n b[n].g[2p - n] \quad (2)$$

$$A_1[k] = \sum_n b[n].h[2p - n] \quad (3)$$

where in (2) and (3), D_1 and A_1 are the first level of detail and approximation coefficients, respectively and p and n are the scaling and translation parameters, respectively. In the current study, the 5th decomposition level of Daubechies wavelet transform is applied to b and the last detail coefficients (D_5) is extracted for reducing the size of the features and make a tradeoff between the time and frequency resolution [38]. The adoption of the Daubechies wavelet is motivated by its exceptional equilibrium between temporal and frequency localization, rendering it well-suited for the detection of transitory attributes such as EEG signal [56], [57]. The attribute D_5 is correlated with the frequency range of 8 to 16 Hz, proving to be a highly advantageous choice for the examination of SSVEP specifically at 15 Hz. Following calculating the D_5 for each channel, they are concatenated to apply as the input to the classifier ($D_{total} = [D_{5,1}; D_{5,2}; D_{5,3}; \ldots; D_{5,10}]$). The maximum iteration of $n = 20$ was selected heuristically for updating the weights in the fast ICA-FBCCA algorithm. The number of sub-bands in the filer bank is considered as five according to [25]. The low and high frequency cut-off were designed as: (10,16) Hz, (16,22) Hz, (24,30) Hz, (32,38) Hz and (40,46) Hz [25] for both datasets.

2) CLASSIFIER

CNN is one of the most common DNN models used in image and video recognition [58], [59], recommender systems [60], image classification [61], natural language processing [62], and particularly SSVEP-based BCI [41], [49], [50], [51]. In the current study, CNN is applied as a robust classifier to the input features (explained in the feature extraction section) for recognizing the targets. As shown in Fig. 2, the proposed CNN contains four layers: two batch normalization (BN) layers, a temporal convolutional layer, and a fully connected softmax classification layer. A BN layer is applied to the input feature space, and subsequently, a total of 50 filters with a size of 1×30 for Dataset 1 and 80 filters with a size of 1×70 for Dataset 2 is convolved into the output of the first BN layer, with stride sizes of 1 in each dimension. It is worth noting that the input sizes of the proposed CNN vary across different feature extraction methods which may lead to change the final performance. Nevertheless, based on our prior analyses and experiments, there is no substantial variance in the results obtained using various parameters optimized for the specific structure of the proposed CNN. Therefore, the filter size and the number of filters are heuristically determined to

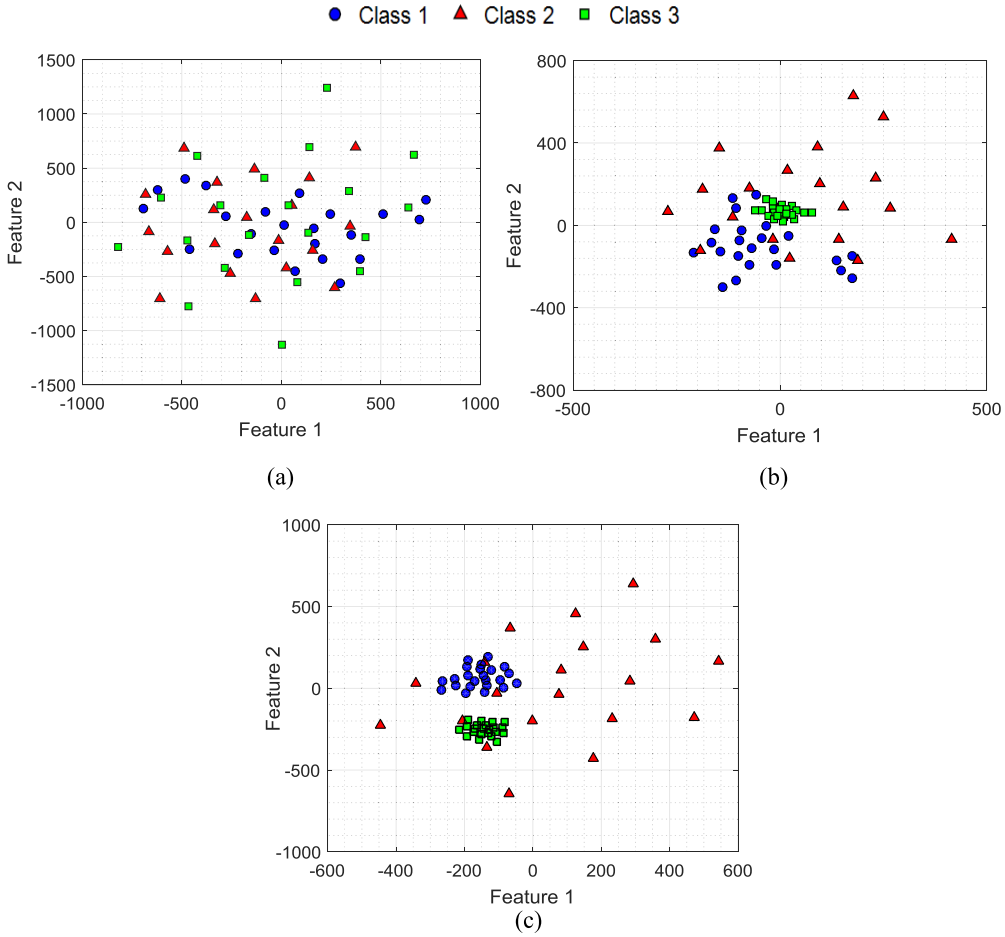

FIGURE 3. The t-SNE visualization illustrating the distribution of the two most discriminative features obtained using three distinct methods for Dataset 1. The methods include: (a) preprocessed step involving filtering and segmentation, (b) fast ICA-FBCCA, and (c) fast ICA-FBCCA-DWT. The visualization showcases their application across three classes.

optimize classification performance for different extraction methods and then fixed throughout the experiments to obtain the results. The convolutional layer uses kernels to capture structural information of the input data automatically which are calculated as follows [63]:

$$x^l = m(x^{l-1} * w^l + b^l) \tag{4}$$

where x^{l-1} is the input of the layer l, x^l is the feature map of the layer l, w^l is the connecting weight, b^l is the offset of features of layer l, and m is the activation function which introduces nonlinearity to the NN. Following the temporal convolutional layer, a second BN layer is employed to diminish the covariate shift of the feature maps. The output of this layer undergoes a nonlinear Rectified Linear Unit (ReLU) activation function, which activates neurons with positive inputs while returning 0 for negative values. Subsequently, the features are flattened and linked to a fully connected layer, serving as an N (number of classes) hidden NN with N output neurons ($N = 3$ and 4 for Dataset 1 and Dataset 2, respectively). In the concluding layer of the network, the softmax activation function assigns probabilities to each output of the fully connected layer. The softmax function takes an input vector $p = (p_0, \ldots p_k)$ in a c-class problem and computes the probability of each class i as follows:

$$\sigma(\vec{p})_i = \frac{e^{p_i}}{\sum_{j=1}^{c} e^{p_j}}, i = 1, \ldots, N \tag{5}$$

This equation shows how the softmax function normalizes the exponentials of the input values to produce meaningful predictions that sum up to 1.

III. RESULTS

The performance of the proposed algorithm is evaluated using two single-flicker SSVEP datasets and the results are compared with the previous work [20], [56]. To evaluate the performance of the proposed algorithm, 3-fold and 5-fold cross-validation was utilized for the Dataset 1 according to [56] and Dataset 2, respectively. The final 15 percent of train data was used for the validation.

A. RESULTS OF DATASET 1

The t-Stochastic Neighbor Embedding (T-SNE) is designed to optimize the pairwise distances of data points in a reduced space to match the distances in the original manifold. The

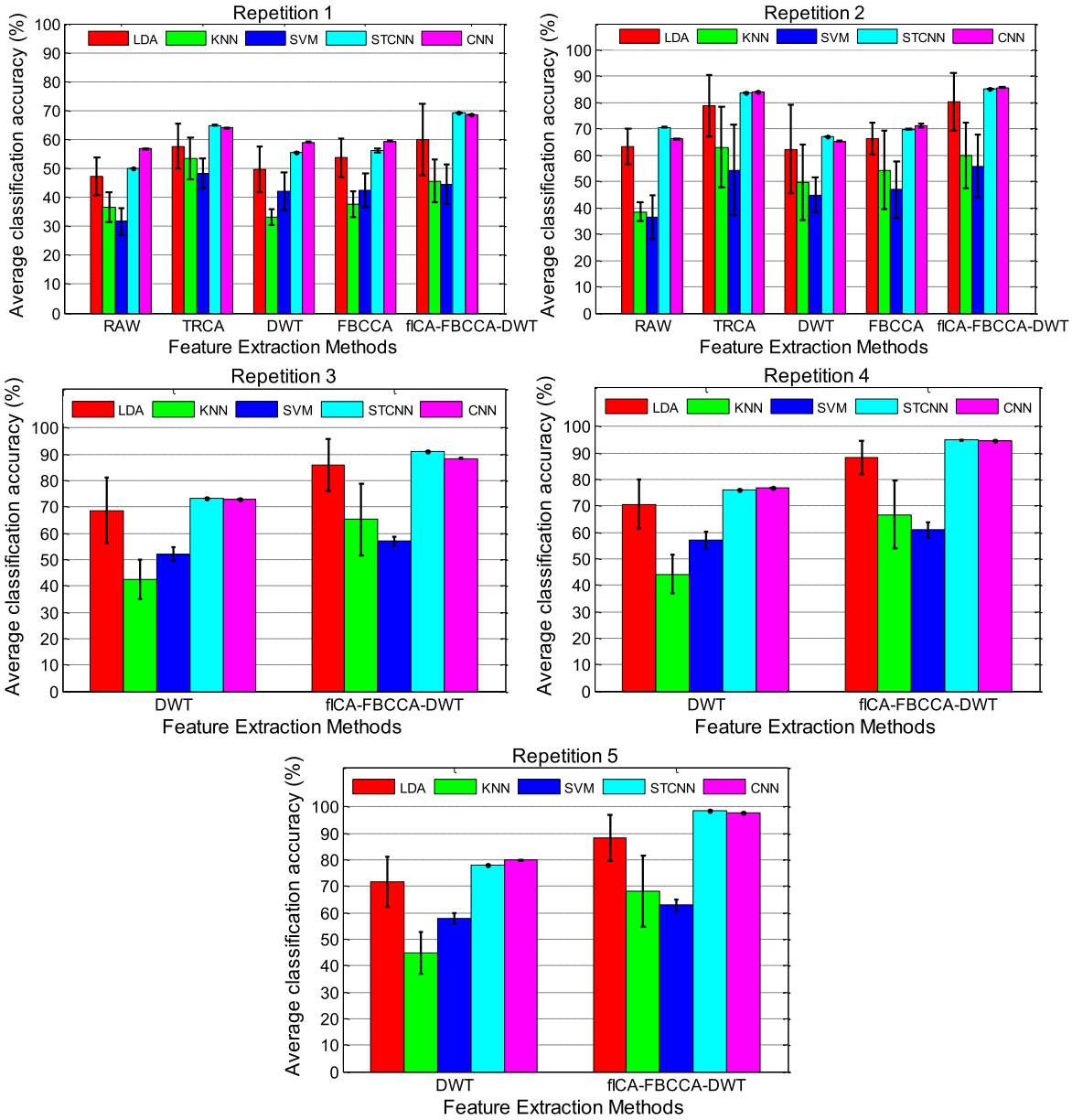

FIGURE 4. The average classification accuracy rates for Dataset 1 across all subjects, considering various classifiers and feature extraction methods over five repetitions. The term "flCA" denotes the fast ICA method.

method is a powerful visualization technique that facilitates the mapping of data points from high-dimensional spaces to lower-dimensional spaces, typically two or three dimensions (2D or 3D) [64]. In our case, we sought to represent each point in a 2D space to better visualize the impact of our proposed method. As depicted in Fig. 3, the features of different classes were more distinguishable in fast ICA-FBCCA-DWT when compared to both fast ICA-FBCCA and preprocessed data. Furthermore, the features of the classes learned by fast ICA-FBCCA were more distinct in comparison with those of the preprocessed data. Additionally, when measuring the correlation between the two most discriminative features, fast ICA-FBCCA-DWT achieved a p-value of 0.02 (t-test), compared to 0.16 for fast ICA-FBCCA and 0.56 for the preprocessed step (which involved segmentation and filtering).

This study aims to evaluate the performance of fast ICA-FBCCA-DWT in comparison with the other feature extraction algorithms including FBCCA [25], task related component analysis (TRCA) [65], and DWT [38], applied to different classifiers such as linear discriminant analysis (LDA) [66], support vector machine (SVM) [67], K-NN [68], and spatial-temporal CNN (STCNN). The STCNN architecture incorporates a batch normalized layer, followed by two convolutional layers. The first convolution layer performs convolution across the spatial domain with a kernel dimension of [number of channels$\times$1] and a stride of 1, while the second layer performs convolution across the time domain with a

Algorithm 1 Fast ICA-FBCCA

Input:

- A set of EEG signal $X \in R^{Ch \times T}$, where Ch and T are the number of channels and temporal samples, respectively.
- A set of reference signals by the sinusoidal cosine of 15 Hz $Y \in R^{10 \times T}$.
- The number of iterations n.
- The number of sub-bands in the filter bank fb.

Initialization:

- Set $W = randn(Ch, Ch)$
- Normalize W: $W = \frac{W}{norm(W)}$

for $i = 1 : ch$ **do**
  for $m = 1 : n$ **do**
    $y = W_i^T X$;
    $g = tanh(y)$;
    $tialg = 1 - g^2$;
    $W_i = Xg^T - E(tialg)W_i$;
    if $i > 1$ **do**
    $W_i = W_i - \sum_{j=1}^{i-1} W_j^T W_j W_j$
    end
    $W_i = \frac{W_i}{norm(W_i)}$;
  end
end
$\tilde{X} = WX$;
for j = 1: fb do
  $[V(j), B] =$ canoncorr $(\tilde{X}, Y)$
end

- canoncorr $(\tilde{X}, Y)$ finds optimal V and B which maximize $V \times \tilde{X}$ and $B \times Y$
- Concatenate the V in line j and achieve $\tilde{V}$.

Output: W, $\tilde{V}$.

Note: canoncorr () is a MATLAB function

kernel dimension of 1×30 and a stride of 1. Both convolutional layers have 50 kernels. Fig. 4 displays the average classification accuracy for the aforementioned algorithms. Because of memory constraint, we limited our comparisons to one or two repetitions. However, we performed five repetitions using fast ICA-FBCCA-DWT with all classifiers. Additionally, due to its low-dimensional features and minimal computational burden in classifiers, we employed DWT features for all repetitions. The results illustrate that the proposed fast-ICA-FBCCA-DWT outperforms all other algorithms across all classifiers. Although both the TRCA and our proposed feature extraction method (fast ICA-FBCCA-DWT) demonstrated closely aligned results during the second repetition, a notable disparity emerged in the first repetition. In this instance, our method exhibited an appreciable accuracy enhancement of approximately 5%. Unfortunately, due to the substantial computational demands associated with the TRCA, we encountered space limitations within MATLAB, precluding us from conducting additional repetitions to further explore its performance. Both STCNN and CNN produce similar results, as evidenced by a t-test, which did not reveal any significant differences between the two types of CNN when using our proposed feature extraction method (p-value < 0.05). However, the proposed CNN has fewer parameters than STCNN, making it more suitable for real-time implementation. Table 1 summarizes the average of accuracy over six subjects using the proposed Fast ICA-FBCCA-DWT+CNN (Fast ICA-FBCCA-DWT as the feature extraction and CNN as the classifier) algorithm for the single-flicker SSVEP in comparison with the results reported in [56] and FBCCA+CNN, DWT+CNN, TRCA+CNN, and RAW+CNN methods, which is consistent with those presented in Fig. 4. These results clearly indicate that the proposed method achieves high classification accuracy across all repetitions ($p \leq 0.05$ for repetitions 1-5) in comparison with the DWT+CNN method.

Fig. 5 shows the average classification accuracy over six subjects using the proposed fast ICA-FBCCA-DWT+CNN

TABLE 1. The average of accuracy (± one standard deviation) over six subjects using the proposed Fast ICA-FBCCA-DWT+CNN algorithm for the Dataset 1 in comparison with the results reported in [56] and FBCCA+CNN, DWT+CNN, TRCA+CNN, and RAW+CNN. The cells of the table with "-" indicate that no analysis was performed.

Feature extraction method	Number of repetitions				
	1	2	3	4	5
	Average of SSVEP accuracy (%)				
Fast ICA-FBCCA-DWT+CNN (proposed)	70.4 ± 13.3	85.6 ± 7.5	91.4 ± 4.1	95 ± 4	97 ± 3.1
FBCCA+CNN	59.4 ± 3.0	71.1 ± 4.4	-	-	-
DWT+CNN	59 ± 2.5	65.2 ± 4.7	72.9 ± 2.7	76.8 ± 2.0	80 ± 3.5
TRCA+CNN	63.9 ± 2.2	84 ± 3.6	-	-	-
RAW+CNN	56.7 ± 4.3	66.2 ± 5.3	-	-	-
[56]	47.88	73.61	87.5	93.06	96.75
Method comparison	**Number of repetitions**				
	1	2	3	4	5
	p-value				
FBCCA+CNN vs. Fast ICA-FBCCA-DWT+CNN	*	*	-	-	-
DWT+CNN vs. Fast ICA-FBCCA-DWT+CNN	*	*	*	*	*
TRCA+CNN vs. Fast ICA-FBCCA-DWT+CNN	*	*	-	-	-
RAW+CNN vs. Fast ICA-FBCCA-DWT+CNN	*	*	-	-	-

*: $p \leq 0.05$

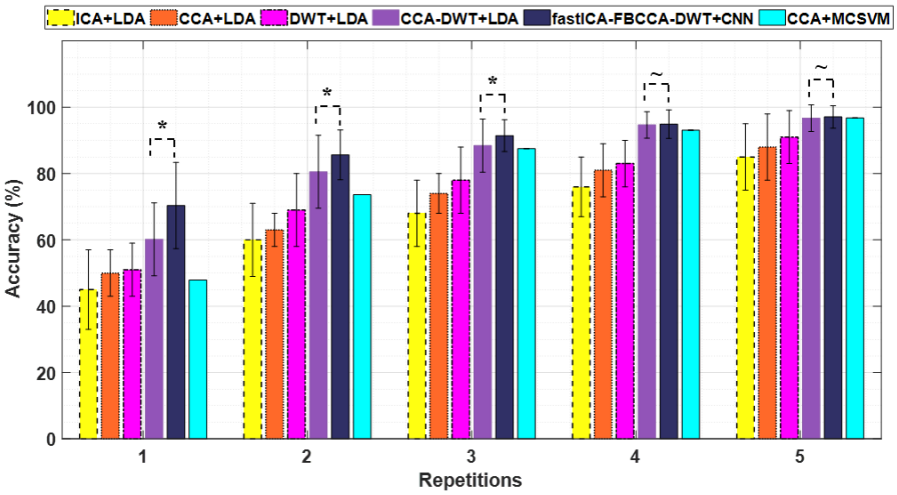

FIGURE 5. The average classification accuracy for Dataset 1 over six subjects, contrasting the performance of the fast ICA-FBCCA-DWT+CNN approach with previously reported results from ICA+LDA [69], CCA+LDA [69], CCA-DWT+LDA [69], CCA+MCSVM [56] on this dataset. Note: ∼nonsignificant, *$p < 0.05$.

compared with the previous works that reported their results on this dataset including the ICA+LDA [69], CCA+LDA [69], DWT+LDA [69], CCA-DWT+LDA [69], and CCA+multi-class kernel SVM (MCSVM) [56] techniques. All analysis in previous studies used 3-fold cross validation for this dataset. The *t*-test results indicate that top average classification performance was achieved for three first repetitions with *p*-value < 0.05, 0.008, and 0.03, respectively. However, although the fast ICA-FBCCA-DWT+CNN achieved higher performance compared to ICA+LDA, CCA+LDA and DWT+LDA in two last repetitions, there is no significant results compared to the CCA-DWT+LDA in repetitions 4 and 5. In BCI-based applications, achieving higher performance in low repetitions is a critical issue, because this is caused by the increasing the speed of BCI-based systems that are in line with real-time implementation.

B. RESULTS OF DATASET 2

In this section, we focused on evaluating the outcomes of our proposed method, known as fast ICA-FBCCA-DWT+CNN, across a cohort of 12 subjects. This method

TABLE 2. The average of accuracy (± one standard deviation) over 12 subjects using the proposed FAST ICA-FBCCA-DWT+CNN algorithm for dataset 2 in comparison with the results of CCA+CNN, FBCCA+CNN, and TRCA+CNN.

Methods	Subjects												Average
	1	2	3	4	5	6	7	8	9	10	11	12	
fICA-FBCCA-DWT+CNN (Proposed method)	81.5	98.5	81.25	90.5	75.5	85.75	93.25	85.5	79.25	63.75	63	88	82.1 ± 10.7
FBCCA+CNN	82	92.7	76.5	74	70.7	81.2	85	74.7	63.2	67.7	55	86	75.7 ± 10.5
CCA+CNN	67	94.2	67.5	82.7	59.2	77.2	78	61	67	60.2	46.7	76.7	69.7 ± 12.6
TRCA+CNN	70	86.5	80.5	77.5	55.5	69	68.5	62.5	58.5	56.5	67	68	68.3 ± 9.5

was compared against several other techniques include CCA+CNN, FBCCA+CNN, and TRCA+CNN. These results are comprehensively summarized in Table 2, presenting an overview of the achieved accuracy. For more evaluation we applied the t-test conducted between the proposed method results with other compared method. These results were confirming the superiority of our proposed approach with all compared methods ($p < 0.005$). Moreover, we conducted a statistical t-test to compare the results of FBCCA+CNN with those of TRCA+CNN and CCA+CNN. The analysis revealed noteworthy distinctions between these methods, with a significance level of $p < 0.05$. This underscores the superior performance of FBCCA in the context of this specific dataset focused on single flicker SSVEP.

IV. DISCUSSION AND CONCLUSION

ML methods are crucial for EEG-based BCI systems, as they establish a connection between mental intentions and external commands. The process entails capturing brain signals, transmitting them to a computer, and subsequently employing ML techniques to categorize the intended target for the purpose of enabling control or communication. These systems are particularly useful for neuromuscular patients who are unable to use their muscles to operate rehabilitation tools. ML-based BCI systems have various applications, including device control for wheelchairs, robots, and spellers. However, a significant challenge in SSVEP-based BCI systems is the problem of eye fatigue. To overcome this issue, the single-flicker SSVEP approach was introduced, but there is currently no suitable analysis available for this type of signal because it is a new approach in the field of BCI systems, especially in speller-based BCI. In the current study, we especially focus on the design of the new feature extraction algorithm based on fast ICA-FBCCA and DWT to extract the robust features from the single-flicker SSVEP signal. The fast ICA-FBCCA-DWT+CNN method increased the accuracy of the first and two repetitions (Table 1 and Fig. 4). By achieving suitable performance with few repetitions, we address a critical challenge in the field. This improves the efficiency of EEG-based tasks and data collection and alleviates participant fatigue. Therefore, this makes our research suitable for practical implementation.

Generally, single-flicker SSVEP is analyzed based on spatial information of the brain. The authors in [56] analyzed the single-flicker SSVEP signal using traditional methods based on the CCA technique (which is based on extracting the spatial features) for feature extraction and the SVM for classification. However, they could not obtain a high accuracy of classification useful in real-time BCI applications in the small number of the repetitions (especially first repetition). This motivated us to develop a CNN-based classification approach in addition to introduce the feature extraction method. This is the first application of DNNs according to our knowledge for analysis of single-flicker SSVEP signals. Although the temporal information of EEG signals represents the nonlinear dynamics and nonstationary processes of EEG and the spatial information captures the dependencies among electrodes or brain regions, the study [70] suggested that temporal signals carry spatial information. Therefore inspired by the [70], we have limited our approach to extracting the optimal spatial features in the feature extraction technique and have considered only convolutional temporal layers in the classification. The previous works [41], [49], [51] utilized both temporal and spatial convolutional layers embedded in the complicated structure of the CNN. However, we developed a FBCCA-based approach which is a powerful spatial filter for the analysis of single-flicker SSVEP as the input to a temporal convolutional layer without requiring to the spatial layer. Fig. 4 demonstrated suitable results of our proposed CNN compared to a STCNN including two convolutional layers (one spatial layer and one temporal layer), respectively. One problem that should be considered in a real-time BCI application is obtaining high performance with small training data. In the structure of the STCNN, due to the large number of parameters to be adjusted, the network requires more training data for achieving high performance which limits the real-time implementation because of the increased calibration time from recording more training data. Moreover, in [62] several fully connected layers with more tunable parameters have been utilized. In contrast, in the current paper, to reduce the number of adjusted parameters in the training phase and to prevent overfitting, only one fully connected layer with three neurons (corresponding to three classes) was considered as the output layer.

V. LIMITATIONS AND FUTURE WORK

While the single-flicker SSVEP paradigm holds promise for BCI applications, our study has certain limitations that suggests potential avenues for future research. Firstly, it is

important to note that the utilization of a single-flicker frequency introduces a constraint on the number of selectable targets, potentially restricting the scope of more complex BCI applications. In future work, expanding the paradigm to encompass multiple-flicker frequencies could address this limitation and enable a broader range of target selections. This can be achieved by incorporating a hybrid approach, such as integrating the P300 or motor imagery paradigms with the single-flicker SSVEP. Additionally, although some BCI literature such as [71] and [72] used several subjects in their study, our evaluation process was impeded by the lack of available state-of-the-art datasets that align precisely with the parameters of the study. This limitation could be overcome in subsequent research by either generating purpose-designed datasets or collaborating with other researchers to acquire suitable data for comprehensive evaluation. Furthermore, while the single-flicker SSVEP paradigm presents advantages in terms of reduced eye fatigue compared to its multiple-flicker counterpart, it is not impervious to the influence of noise and artifacts originating from eye movements, muscle activity, and external factors. The impact of these sources of interference on the reliability and consistency of the SSVEP signal warrants further investigation. This can be accomplished by creating techniques to reduce signal noise or by comparing various denoising methods, such as principal component analysis (PCA), common spatial pattern (CSP), and their combinations. Future studies could focus on refining signal processing techniques [73], [74], [75], possibly incorporating advanced noise reduction methods [76], [77], [78] or adaptive filtering algorithms to enhance the signal quality and robustness. In addition to the above limitations, in the current study, we used FBCCA algorithm as a powerful spatial filter for the analysis of single-flicker SSVEP. But, FBCCA has a higher computational cost in comparison with the standard CCA method, because it uses multiple filters and weights to process the SSVEP signals. However, FBCCA can achieve better performance than CCA by capturing more frequency components of SSVEPs. In our work, we used only 5 sub-band, which reduced the computational cost of FBCCA while maintaining a performance level close to that of traditional CCA. Nevertheless, there are several spatial filters which could potentially contribute to the overall performance improvement. Exploring the efficacy of these spatial filters in the context of our single-flicker SSVEP paradigm remains an area of potential exploration in future research. Moreover, it is worth noting that our proposed method necessitates a training signal for model calibration. This training requirement could present challenges in real-time scenarios, where rapid adaptability is crucial. To mitigate this limitation, future investigations could explore the use of transfer-learning techniques, which could allow the model to adjust more effectively to novel users or scenarios with minimal retraining. This technique leverages the knowledge learned from a source domain to improve the performance on a target domain and reducing the need for large amounts of labeled data. Such techniques could also improve the generalization and robustness of the model across different domains and tasks.

REFERENCES

[1] X. Wan, K. Zhang, S. Ramkumar, J. Deny, G. Emayavaramban, M. S. Ramkumar, and A. F. Hussein, "A review on electroencephalogram based brain computer interface for elderly disabled," *IEEE Access*, vol. 7, pp. 36380–36387, 2019, doi: 10.1109/ACCESS.2019.2903235.

[2] R. Abiri, S. Borhani, E. W. Sellers, Y. Jiang, and X. Zhao, "A comprehensive review of EEG-based brain–computer interface paradigms," *J. Neural Eng.*, vol. 16, no. 1, Feb. 2019, Art. no. 011001, doi: 10.1088/1741-2552/aaf12e.

[3] W. Chen, S.-K. Chen, Y.-H. Liu, Y.-J. Chen, and C.-S. Chen, "An electric wheelchair manipulating system using SSVEP-based BCI system," *Biosensors*, vol. 12, no. 10, pp. 1–20, Sep. 2022, doi: 10.3390/bios12100772.

[4] A. F. P. Vidal, M. A. O. Salazar, and G. S. Lopez, "Development of a brain–computer interface based on visual stimuli for the movement of a robot joints," *IEEE Latin Amer. Trans.*, vol. 14, no. 2, pp. 477–484, Feb. 2016, doi: 10.1109/TLA.2016.7437182.

[5] Y. Lu, L. Bi, J. Lian, and H. Li, "Mathematical modeling of EEG signals-based brain-control behavior," *IEEE Trans. Neural Syst. Rehabil. Eng.*, vol. 26, no. 8, pp. 1535–1543, Aug. 2018, doi: 10.1109/TNSRE.2018.2855263.

[6] J. Long, Y. Li, T. Yu, and Z. Gu, "Target selection with hybrid feature for BCI-based 2-D cursor control," *IEEE Trans. Biomed. Eng.*, vol. 59, no. 1, pp. 132–140, Jan. 2012, doi: 10.1109/TBME.2011.2167718.

[7] A. Rezeika, M. Benda, P. Stawicki, F. Gembler, A. Saboor, and I. Volosyak, "Brain–computer interface spellers: A review," *Brain Sci.*, vol. 8, no. 4, pp. 1–38, Mar. 2018, doi: 10.3390/brainsci8040057.

[8] G. R. Müller-Putz and G. Pfurtscheller, "Control of an electrical prosthesis with an SSVEP-based BCI," *IEEE Trans. Biomed. Eng.*, vol. 55, no. 1, pp. 361–364, Jan. 2008, doi: 10.1109/TBME.2007.897815.

[9] M. Middendorf, G. Mcmillan, G. Calhoun, and K. S. Jones, "Brain–computer interfaces based on the steady-state visual-evoked response," *IEEE Trans. Rehabil. Eng.*, vol. 8, no. 2, pp. 211–214, Jun. 2000, doi: 10.1109/86.847819.

[10] R. Fazel-Rezai, B. Z. Allison, C. Guger, E. W. Sellers, S. C. Kleih, and A. Kübler, "P300 brain computer interface: Current challenges and emerging trends," *Frontiers Neuroeng.*, vol. 5, no. 14, pp. 1–14, 2012, doi: 10.3389/fneng.2012.00014.

[11] S. N. Aghili, S. Kilani, R. N. Khushaba, and E. Rouhani, "A spatial-temporal linear feature learning algorithm for P300-based brain–computer interfaces," *Heliyon*, vol. 9, no. 4, Apr. 2023, Art. no. e15380, doi: 10.1016/j.heliyon.2023.e15380.

[12] N. P. M. Todd and C. S. Lee, "The sensory-motor theory of rhythm and beat induction 20 years on: A new synthesis and future perspectives," *Frontiers Hum. Neurosci.*, vol. 9, no. 444, pp. 1–25, 2015, doi: 10.3389/fnhum.2015.00444.

[13] T. Hinterberger, S. Schmidt, N. Neumann, J. Mellinger, B. Blankertz, G. Curio, and N. Birbaumer, "Brain–computer communication and slow cortical potentials," *IEEE Trans. Biomed. Eng.*, vol. 51, no. 6, pp. 1011–1018, Jun. 2004, doi: 10.1109/TBME.2004.827067.

[14] A. Rezeika, M. Benda, P. Stawicki, F. Gembler, A. Saboor, and I. Volosyak, "Brain–computer interface spellers: A review," *Brain Sci.*, vol. 8, no. 4, p. 57, Mar. 2018, doi: 10.3390/brainsci8040057.

[15] D. Zhang, A. Maye, X. Gao, B. Hong, A. K. Engel, and S. Gao, "An independent brain–computer interface using covert non-spatial visual selective attention," *J. Neural Eng.*, vol. 7, no. 1, Feb. 2010, Art. no. 016010, doi: 10.1088/1741-2560/7/1/016010.

[16] X. Gao, D. Xu, M. Cheng, and S. Gao, "A BCI-based environmental controller for the motion-disabled," *IEEE Trans. Neural Syst. Rehabil. Eng.*, vol. 11, no. 2, pp. 137–140, Jun. 2003, doi: 10.1109/TNSRE.2003.814449.

[17] Y. Punsawad and Y. Wongsawat, "Multi-command SSAEP-based BCI system with training sessions for SSVEP during an eye fatigue state," *IEEJ Trans. Electr. Electron. Eng.*, vol. 12, no. S1, pp. S72–S78, Jun. 2017, doi: 10.1002/tee.22441.

[18] C. Liu, J. Wang, H. Li, M. Lu, B. Deng, H. Yu, X. Wei, C. Fietkiewicz, and K. A. Loparo, "Closed-loop modulation of the pathological disorders of the basal ganglia network," *IEEE Trans. Neural Netw. Learn. Syst.*, vol. 28, no. 2, pp. 371–382, Feb. 2017.

[19] A. Maye, D. Zhang, and A. K. Engel, "Utilizing retinotopic mapping for a multi-target SSVEP BCI with a single flicker frequency," *IEEE Trans. Neural Syst. Rehabil. Eng.*, vol. 25, no. 7, pp. 1026–1036, Jul. 2017, doi: 10.1109/TNSRE.2017.2666479.

[20] J. Chen, D. Zhang, A. K. Engel, Q. Gong, and A. Maye, "Application of a single-flicker online SSVEP BCI for spatial navigation," *PLoS ONE*, vol. 12, no. 5, May 2017, Art. no. e0178385, doi: 10.1371/journal.pone.0178385.

[21] Y. Punsawad and Y. Wongsawat, "A multi-command SSVEP-based BCI system based on single flickering frequency half-field steady-state visual stimulation," *Med. Biol. Eng. Comput.*, vol. 55, no. 6, pp. 965–977, Jun. 2017, doi: 10.1007/s11517-016-1560-3.

[22] J. Chen, A. Maye, A. K. Engel, Y. Wang, X. Gao, and D. Zhang, "Simultaneous decoding of eccentricity and direction information for a single-flicker SSVEP BCI," *Electronics*, vol. 8, no. 12, pp. 1–13, Dec. 2019, doi: 10.3390/electronics8121554.

[23] Z. Lin, C. Zhang, W. Wu, and X. Gao, "Frequency recognition based on canonical correlation analysis for SSVEP-based BCIs," *IEEE Trans. Biomed. Eng.*, vol. 54, no. 6, pp. 1172–1176, Jun. 2007, doi: 10.1109/TBME.2006.889197.

[24] Y. Li, J. Xiang, and T. Kesavadas, "Convolutional correlation analysis for enhancing the performance of SSVEP-based brain–computer interface," *IEEE Trans. Neural Syst. Rehabil. Eng.*, vol. 28, no. 12, pp. 2681–2690, Dec. 2020, doi: 10.1109/TNSRE.2020.3038718.

[25] X. Chen, Y. Wang, S. Gao, T.-P. Jung, and X. Gao, "Filter bank canonical correlation analysis for implementing a high-speed SSVEP-based brain–computer interface," *J. Neural Eng.*, vol. 12, no. 4, Aug. 2015, Art. no. 046008.

[26] J. A. Urigüen and B. Garcia-Zapirain, "EEG artifact removal—State-of-the-art and guidelines," *J. Neural Eng.*, vol. 12, no. 3, Jun. 2015, Art. no. 031001, doi: 10.1088/1741-2560/12/3/031001.

[27] A. Schlögl, C. Keinrath, D. Zimmermann, R. Scherer, R. Leeb, and G. Pfurtscheller, "A fully automated correction method of EOG artifacts in EEG recordings," *Clin. Neurophysiol.*, vol. 118, no. 1, pp. 98–104, Jan. 2007, doi: 10.1016/j.clinph.2006.09.003.

[28] S. Casarotto, A. M. Bianchi, S. Cerutti, and G. A. Chiarenza, "Principal component analysis for reduction of ocular artefacts in event-related potentials of normal and dyslexic children," *Clin. Neurophysiol.*, vol. 115, no. 3, pp. 609–619, Mar. 2004, doi: 10.1016/j.clinph.2003.10.018.

[29] M. T. Akhtar, W. Mitsuhashi, and C. J. James, "Employing spatially constrained ICA and wavelet denoising, for automatic removal of artifacts from multichannel EEG data," *Signal Process.*, vol. 92, no. 2, pp. 401–416, Feb. 2012, doi: 10.1016/j.sigpro.2011.08.005.

[30] L. Albera, A. Kachenoura, P. Comon, A. Karfoul, F. Wendling, L. Senhadji, and I. Merlet, "ICA-based EEG denoising: A comparative analysis of fifteen methods," *Bull. Polish Acad. Sci., Tech. Sci.*, vol. 60, no. 3, pp. 407–418, Dec. 2012, doi: 10.2478/v10175-012-0052-3.

[31] S. Hoffmann and M. Falkenstein, "The correction of eye blink artefacts in the EEG: A comparison of two prominent methods," *PLoS ONE*, vol. 3, no. 8, p. e3004, Aug. 2008, doi: 10.1371/journal.pone.0003004.

[32] W. Zhou and J. Gotman, "Automatic removal of eye movement artifacts from the EEG using ICA and the dipole model," *Prog. Natural Sci.*, vol. 19, no. 9, pp. 1165–1170, Sep. 2009, doi: 10.1016/j.pnsc.2008.11.013.

[33] Y. Li, Z. Ma, W. Lu, and Y. Li, "Automatic removal of the eye blink artifact from EEG using an ICA-based template matching approach," *Physiol. Meas.*, vol. 27, no. 4, pp. 425–436, Apr. 2006, doi: 10.1088/0967-3334/27/4/008.

[34] A. Hyvarinen, "Fast and robust fixed-point algorithms for independent component analysis," *IEEE Trans. Neural Netw.*, vol. 10, no. 3, pp. 626–634, May 1999.

[35] B. W. Mcmenamin, A. J. Shackman, L. L. Greischar, and R. J. Davidson, "Electromyogenic artifacts and electroencephalographic inferences revisited," *NeuroImage*, vol. 54, no. 1, pp. 4–9, Jan. 2011, doi: 10.1016/j.neuroimage.2010.07.057.

[36] W. De Clercq, A. Vergult, B. Vanrumste, W. Van Paesschen, and S. Van Huffel, "Canonical correlation analysis applied to remove muscle artifacts from the electroencephalogram," *IEEE Trans. Biomed. Eng.*, vol. 53, no. 12, pp. 2583–2587, Nov. 2006, doi: 10.1109/TBME.2006.879459.

[37] K. T. Sweeney, S. F. McLoone, and T. E. Ward, "The use of ensemble empirical mode decomposition with canonical correlation analysis as a novel artifact removal technique," *IEEE Trans. Biomed. Eng.*, vol. 60, no. 1, pp. 97–105, Jan. 2013, doi: 10.1109/TBME.2012.2225427.

[38] N. Robinson, A. P. Vinod, K. K. Ang, K. P. Tee, and C. T. Guan, "EEG-based classification of fast and slow hand movements using wavelet-CSP algorithm," *IEEE Trans. Biomed. Eng.*, vol. 60, no. 8, pp. 2123–2132, Aug. 2013, doi: 10.1109/TBME.2013.2248153.

[39] N. K. Nik Aznan, S. Bonner, J. Connolly, N. Al Moubayed, and T. Breckon, "On the classification of SSVEP-based dry-EEG signals via convolutional neural networks," in *Proc. IEEE Int. Conf. Syst., Man, Cybern. (SMC)*, Oct. 2018, pp. 3726–3731, doi: 10.1109/SMC.2018.00631.

[40] J. Thomas, T. Maszczyk, N. Sinha, T. Kluge, and J. Dauwels, "Deep learning-based classification for brain–computer interfaces," in *Proc. IEEE Int. Conf. Syst., Man, Cybern. (SMC)*, Oct. 2017, pp. 234–239, doi: 10.1109/SMC.2017.8122608.

[41] N.-S. Kwak, K.-R. Müller, and S.-W. Lee, "A convolutional neural network for steady state visual evoked potential classification under ambulatory environment," *PLoS ONE*, vol. 12, no. 2, Feb. 2017, Art. no. e0172578, doi: 10.1371/journal.pone.0172578.

[42] J. Marecek, "Handbook of approximation algorithms and metaheuristics," *Comput. J.*, vol. 53, no. 8, pp. 1338–1339, Oct. 2010, doi: 10.1093/comjnl/bxp121.

[43] A. Dhillon and G. K. Verma, "Convolutional neural network: A review of models, methodologies and applications to object detection," *Prog. Artif. Intell.*, vol. 9, no. 2, pp. 85–112, 2020, doi: 10.1007/s13748-019-00203-0.

[44] M. M. Taye, "Theoretical understanding of convolutional neural network: Concepts, architectures, applications, future directions," *Computation*, vol. 11, no. 3, pp. 1–23, 2023, doi: 10.3390/computation11030052.

[45] V. J. Lawhern, A. J. Solon, N. R. Waytowich, S. M. Gordon, C. P. Hung, and B. J. Lance, "EEGNet: A compact convolutional neural network for EEG-based brain–computer interfaces," *J. Neural Eng.*, vol. 15, no. 5, Oct. 2018, Art. no. 056013, doi: 10.1088/1741-2552/aace8c.

[46] Y. R. Tabar and U. Halici, "A novel deep learning approach for classification of EEG motor imagery signals," *J. Neural Eng.*, vol. 14, no. 1, Feb. 2017, Art. no. 016003, doi: 10.1088/1741-2560/14/1/016003.

[47] R. T. Schirrmeister, J. T. Springenberg, L. D. J. Fiederer, M. Glasstetter, K. Eggensperger, M. Tangermann, F. Hutter, W. Burgard, and T. Ball, "Deep learning with convolutional neural networks for EEG decoding and visualization," *Hum. Brain Mapping*, vol. 38, no. 11, pp. 5391–5420, Nov. 2017, doi: 10.1002/hbm.23730.

[48] A. Antoniades, L. Spyrou, C. C. Took, and S. Sanei, "Deep learning for epileptic intracranial EEG data," in *Proc. IEEE 26th Int. Workshop Mach. Learn. Signal Process. (MLSP)*, Sep. 2016, pp. 1–6.

[49] A. Ravi, N. H. Beni, J. Manuel, and N. Jiang, "Comparing user-dependent and user-independent training of CNN for SSVEP BCI," *J. Neural Eng.*, vol. 17, no. 2, Apr. 2020, Art. no. 026028, doi: 10.1088/1741-2552/ab6a67.

[50] T.-H. Nguyen and W.-Y. Chung, "A single-channel SSVEP-based BCI speller using deep learning," *IEEE Access*, vol. 7, pp. 1752–1763, 2019, doi: 10.1109/ACCESS.2018.2886759.

[51] N. Waytowich, V. J. Lawhern, J. O. Garcia, J. Cummings, J. Faller, P. Sajda, and J. M. Vettel, "Compact convolutional neural networks for classification of asynchronous steady-state visual evoked potentials," *J. Neural Eng.*, vol. 15, no. 6, Dec. 2018, Art. no. 066031, doi: 10.1088/1741-2552/aae5d8.

[52] K. Liu, Y. Yu, L.-L. Zeng, X. Liang, Y. Liu, X. Chu, G. Lu, and Z. Zhou, "Effects of low mental energy from long periods of work on brain–computer interfaces," *Brain Sci.*, vol. 12, no. 9, p. 1152, Aug. 2022, doi: 10.3390/brainsci12091152.

[53] W. Liu, H. Jiang, and Y. Lu, "Analyze EEG signals with convolutional neural network based on power spectrum feature selection," *Proc. Sci.*, vol. 2017, pp. 1–7, Jul. 2017, doi: 10.22323/1.299.0002.

[54] M. Liu, W. Wu, Z. Gu, Z. Yu, F. Qi, and Y. Li, "Deep learning based on batch normalization for P300 signal detection," *Neurocomputing*, vol. 275, pp. 288–297, Jan. 2018, doi: 10.1016/j.neucom.2017.08.039.

[55] J. Nagi, F. Ducatelle, G. A. Di Caro, D. Cireşan, U. Meier, A. Giusti, F. Nagi, J. Schmidhuber, L. M. Gambardella, "Max-pooling convolutional neural networks for vision-based hand gesture recognition," in *Proc. IEEE Int. Conf. Signal Image Process. Appl. (ICSIPA)*, Nov. 2011, pp. 342–347.

[56] S. Jalilpour, S. Hajipour Sardouie, and A. Mijani, "A novel hybrid BCI speller based on RSVP and SSVEP paradigm," *Comput. Methods Programs Biomed.*, vol. 187, Apr. 2020, Art. no. 105326, doi: 10.1016/j.cmpb.2020.105326.

[57] Y. Peng, C. M. Wong, Z. Wang, A. C. Rosa, H. T. Wang, and F. Wan, "Fatigue detection in SSVEP-BCIs based on wavelet entropy of EEG," *IEEE Access*, vol. 9, pp. 114905–114913, 2021, doi: 10.1109/ACCESS.2021.3100478.

[58] C. Ding and D. Tao, "Trunk-branch ensemble convolutional neural networks for video-based face recognition," *IEEE Trans. Pattern Anal. Mach. Intell.*, vol. 40, no. 4, pp. 1002–1014, Apr. 2018, doi: 10.1109/TPAMI.2017.2700390.
[59] N. M. Ashraf, R. R. Mostafa, R. H. Sakr, and M. Z. Rashad, "A state-of-the-art review of deep reinforcement learning techniques for real-time strategy games," in *Applications of Artificial Intelligence in Business, Education and Healthcare*. Cham, Switzerland: Springer, 2021, pp. 285–307, doi: 10.1007/978-3-030-72080-3_17.
[60] S. Zhang, L. Yao, A. Sun, and Y. Tay, "Deep learning based recommender system: A survey and new perspectives," *ACM Comput. Surv.*, vol. 52, no. 1, pp. 1–38, Jan. 2020, doi: 10.1145/3285029.
[61] Y. Pei, Y. Huang, Q. Zou, X. Zhang, and S. Wang, "Effects of image degradation and degradation removal to CNN-based image classification," *IEEE Trans. Pattern Anal. Mach. Intell.*, vol. 43, no. 4, pp. 1239–1253, Apr. 2021, doi: 10.1109/TPAMI.2019.2950923.
[62] W. Yin, K. Kann, M. Yu, and H. Schütze, "Comparative study of CNN and RNN for natural language processing," 2017, *arXiv:1702.01923*.
[63] G. B. Kshirsagar and N. D. Londhe, "Improving performance of devanagari script input-based P300 speller using deep learning," *IEEE Trans. Biomed. Eng.*, vol. 66, no. 11, pp. 2992–3005, Nov. 2019, doi: 10.1109/TBME.2018.2875024.
[64] L. Van Der Maaten and G. Hinton, "Visualizing data using t-SNE," *J. Mach. Learn. Res.*, vol. 9, no. 11, pp. 2579–2625, 2008.
[65] M. Nakanishi, Y. Wang, X. Chen, Y.-T. Wang, X. Gao, and T.-P. Jung, "Enhancing detection of SSVEPs for a high-speed brain speller using task-related component analysis," *IEEE Trans. Biomed. Eng.*, vol. 65, no. 1, pp. 104–112, Jan. 2018, doi: 10.1109/TBME.2017.2694818.
[66] S. Balakrishnama and A. Ganapathiraju, "Linear discriminant analysis-a brief tutorial," *Inst. Signal Inf. Process.*, vol. 18, pp. 1–8, 1998.
[67] D. A. Pisner and D. M. Schnyer, *Support Vector Machine*. Amsterdam, The Netherlands: Elsevier, 2019.
[68] H. Salem, M. Y. Shams, O. M. Elzeki, M. A. Elfattah, J. F. Al-Amri, and S. Elnazer, "Fine-tuning fuzzy KNN classifier based on uncertainty membership for the medical diagnosis of diabetes," *Appl. Sci.*, vol. 12, no. 3, pp. 1–26, Jan. 2022, doi: 10.3390/app12030950.
[69] S. N. A. Kordmahale, S. Kilani, Z. Ghassemlooy, Q. Wu, and A. Maleki, "A novel artifact removal method for the SSVEP signal using hybrid CCA-DWT and comparative analysis for feature selection and classification in the P300 signal," in *Proc. 13th Int. Symp. Commun. Syst., Netw. Digit. Signal Process. (CSNDSP)*, Jul. 2022, pp. 390–394, doi: 10.1109/CSNDSP54353.2022.9907961.
[70] E. Su, S. Cai, L. Xie, H. Li, and T. Schultz, "STAnet: A spatiotemporal attention network for decoding auditory spatial attention from EEG," *IEEE Trans. Biomed. Eng.*, vol. 69, no. 7, pp. 2233–2242, Jul. 2022.
[71] M. T. Sadiq, X. Yu, Z. Yuan, M. Z. Aziz, S. Siuly, and W. Ding, "Toward the development of versatile brain–computer interfaces," *IEEE Trans. Artif. Intell.*, vol. 2, no. 4, pp. 314–328, Aug. 2021, doi: 10.1109/TAI.2021.3097307.
[72] X. Yu, M. Z. Aziz, M. T. Sadiq, Z. Fan, and G. Xiao, "A new framework for automatic detection of motor and mental imagery EEG signals for robust BCI systems," *IEEE Trans. Instrum. Meas.*, vol. 70, pp. 1–12, 2021, doi: 10.1109/TIM.2021.3069026.
[73] H. Akbari, M. T. Sadiq, N. Jafari, T. O. O. Jingwei, N. Mikaeilvand, A. Cicone, and S. Serra-Capizzano, "Recognizing seizure using Poincaré plot of EEG signals and graphical features in DWT domain," *Bratislava Med. J.*, vol. 124, no. 1, pp. 12–24, 2023, doi: 10.4149/BLL_2023_002.
[74] M. T. Sadiq, H. Akbari, S. Siuly, Y. Li, and P. Wen, "Alcoholic EEG signals recognition based on phase space dynamic and geometrical features," *Chaos, Solitons Fractals*, vol. 158, May 2022, Art. no. 112036, doi: 10.1016/j.chaos.2022.112036.
[75] H. Akbari, M. T. Sadiq, M. Payan, S. S. Esmaili, H. Baghri, and H. Bagheri, "Depression detection based on geometrical features extracted from SODP shape of EEG signals and binary PSO," *Traitement du Signal*, vol. 38, no. 1, pp. 13–26, Feb. 2021.
[76] M. T. Sadiq, X. Yu, Z. Yuan, and M. Z. Aziz, "Motor imagery BCI classification based on novel two-dimensional modelling in empirical wavelet transform," *Electron. Lett.*, vol. 56, no. 25, pp. 1367–1369, Dec. 2020, doi: 10.1049/el.2020.2509.
[77] M. T. Sadiq, X. Yu, Z. Yuan, M. Z. Aziz, N. U. Rehman, W. Ding, and G. Xiao, "Motor imagery BCI classification based on multivariate variational mode decomposition," *IEEE Trans. Emerg. Topics Comput. Intell.*, vol. 6, no. 5, pp. 1177–1189, Oct. 2022, doi: 10.1109/TETCI.2022.3147030.
[78] M. T. Sadiq, X. Yu, Z. Yuan, F. Zeming, A. U. Rehman, I. Ullah, G. Li, and G. Xiao, "Motor imagery EEG signals decoding by multivariate empirical wavelet transform-based framework for robust brain–computer interfaces," *IEEE Access*, vol. 7, pp. 171431–171451, 2019, doi: 10.1109/ACCESS.2019.2956018.

SEYEDEH NADIA AGHILI was born in Gorgan, Iran, in 1994. She received the B.Sc. degree in electrical engineering from Golestan University (GU), Gorgan, in 2016, and the M.Sc. degree in biomedical engineering-bioelectric from the Iran University of Science and Technology (IUST), Tehran, Iran, in 2020. Her research interests include BCI, machine learning, deep learning, signal processing, transfer learning, digital health, and real-time implementation. She ranked first in the 4th Iranian Brain–Computer Interface Competition, in 2021.

SEPIDEH KILANI received the B.Sc. degree in electronic engineering from Islamic Azad University, South Tehran Branch, Tehran, Iran, in 2017, and the M.Sc. degree in biomedical engineering from the Iran University of Science and Technology, Tehran, in 2021. Her main research interests include biomedical signal processing, machine learning, deep learning, and transfer learning. She ranked first in the 4th Iranian Brain–Computer Interface Competition, in 2021.

EHSAN ROUHANI received the B.Sc. degree in electrical engineering from Shahrekord University, Shahrekord, Iran, in 2006, the M.Sc. degree in biomedical engineering from the Amirkabir University of Technology, Tehran, Iran, in 2009, and the Ph.D. degree in biomedical engineering from the Iran University of Science and Technology, Tehran, in 2018. Since 2018, he has been a Faculty Member with the Isfahan University of Technology, Isfahan, Iran. The principal focus of research is on the robust control of the movement through functional electrical stimulation. His research interests include fuzzy neural network estimator, adaptive and sliding mode control of the neuromusculoskeletal system using intraspinal microstimulation, chaos control, and robust control of nonlinear biological systems.

AMIR AKHAVAN received the B.Sc. degree in electrical engineering from the Isfahan University of Technology, Isfahan, Iran, in 2008, the M.Sc. degree in biomedical engineering from Tarbiat Modares University, Tehran, Iran, in 2011, and the Ph.D. degree in biomedical engineering from the Amirkabir University of Technology, Tehran, in 2017. In 2018, he joined the Biomedical Engineering Group, Isfahan University of Technology. His current research interests include electrical and ultrasound brain stimulation, biomedical signal processing, discriminative sparse representation models, and array signal processing.